Characterization of Coherent Structures in Tokamak Edge Turbulence

S. Benkadda,[1] T. Dudok de Wit,[2] A. Verga,[1] A. Sen,[3] ASDEX team,[4] and X. Garbet[2]

[1]*Turbulence Plasma, URA 773 Centre National de la Recherche Scientifique-Université de Provence, Institut Méditerranéen de Technologie, F-13451 Marseille Cedex 20, France*

[2]*Département de Recherches sur la Fusion Contrôleé/Service de Physique des Plasmas de Fusion-Centre d'Etudes Nucléaires Cadarache, F-13108 Saint-Paul-lez-Durance Cedex, France*

[3]*Institute for Plasma Research, Bhat, Gandhinagar 382424, India*

[4]*Max-Planck-Institut für Plasmaphysik, D-85748 Garching, Germany*

(Received 14 June 1994)

A statistical test for extracting and identifying coherent structures in the scrape-off layer turbulence is used to analyze Langmuir probe data from the ADITYA and ASDEX tokamaks. This method, the biorthogonal decomposition, allows one to characterize large-scale coherent structures in plasma turbulence in an unambiguous manner. It is shown that such structures effectively contribute to radial transport and to intermittency. Results from numerical simulations of turbulence driven by the resistive interchange instability in the scrape-off layer are compared to the observed statistical properties.

PACS numbers: 52.35.Ra, 02.50.Sk, 52.55.Fa

The role played by localized and long-lived structures in plasma turbulence has become an important research issue in the last decades. Both experimental results [1,2] and numerical simulations [3] support the idea of self-organized turbulence in the scrape-off layer (SOL) of tokamak plasmas. The identification of such coherent structures from spatio-temporal turbulence measurements is fundamental for understanding their dynamics and testing their contribution to radial transport. Their extraction, however, has been a challenge problem so far, due to the lack of adequate analysis techniques [4]. It is thus important to provide appropriate statistical tools for extracting the relevant information from experimental data and to give an accurate description of turbulence in a relatively low-dimensional space. In this Letter we report a simultaneous analysis of the space and time dependences of fluctuation data, using a multivariate technique called the biorthogonal decomposition (BD).

The analysis of edge plasma turbulence has traditionally been based on correlation and spectral techniques [5]. Recently, other techniques such as conditional sampling [6] and bispectral analysis [7] have been used to search for self-organized behavior. Although these methods can be extremely powerful, they do not readily provide a statistical test capable of identifying and extracting coherent structures; they either suffer from an arbitrariness in the definition of coherent structures or lack in adequate spatial or temporal resolution. As a result, the experimental evidence for the existence of such structures has remained inconclusive so far. Another shortcoming of these methods is their inability to properly deal with spatio-temporal signals. Indeed, most of them merely proceed with one-dimensional projections of the data and no full spatio-temporal analysis has been reported.

The BD provides an objective test for identifying and extracting coherent structures without an *a priori* specification of their shape or localization. This statistical method has the interesting property to concentrate most of the pertinent dynamics into a few components, thereby allowing a strong reduction in the number of degrees of freedom necessary to describe the data. Its ability to reveal coherent structures will be used to assess the effect of the latter on radial transport and intermittency. The experimental data analyzed in this letter originate from the SOL of ADITYA [8] and ASDEX [9] tokamaks and the simulations data from a model of SOL turbulence driven by the resistive interchange instability [10].

The BD belongs to a class of methods (proper orthogonal decomposition, Karhunen-Loève expansion, and singular value decomposition) that were originally introduced by Lumley in fluid turbulence [11] and has since been used in fluid mechanics [12] and in magnetohydrodynamics (MHD) activity studies [13]. To illustrate the method, we consider a scalar spatio-temporal signal $y(x,t)$ (e.g., ion saturation current or floating potential) whose temporal evolution is measured simultaneously at M different locations. The signal is subsequently sampled and the data are assembled into an $N \times M$ matrix $\mathbf{Y}$, in which the columns are time series. The BD consists in expanding the discrete data $Y_{ij} = y(x_j, t_i)$ into a unique set of modes that are orthonormal in time and in space, i.e., $Y_{ij} = \sum_{n=1}^{K} A_n v_n(t_i) u_n(x_j)$, where $K = \min(N, M)$ is the finite global dimension of the data set. The base functions $u_n(x_j)$ and $v_n(t_i)$ are, respectively, eigensolutions of the two point temporal and spatial cross-correlation matrices of $\mathbf{Y}$. The weights A_n are either positive or equal to zero, and it is conventional to sort the series in decreasing weight order.

The BD, like other proper orthogonal decomposition methods, is based on a diagonalization of the data cross-correlation matrices. Note that we have a one-to-one correspondence between the spatial and temporal modes, $\mathbf{Y}u_n = A_n v_n$, which corresponds to a dispersion relation. A physical interpretation which stems from these defini-

tions is that the BD projects the data on an orthonormal basis which separates the temporal and the spatial dynamics. Coherent structures that are highly correlated in time or in space appear in heavily weighted components (A_n is large). Traveling waves appear in pairs of components that have equal weights. The more redundant the data set is, the steeper the weight distribution is; totally uncorrelated signals such as random noise will give $A_1 \cong A_2 \cong \cdots \cong A_K$.

In the present Letter we apply the BD to spatio-temporal Langmuir probe data and to 2D simulation data of SOL turbulence. The experimental density fluctuations $\tilde{n}$ are inferred from the ion saturation current and the potential fluctuations $\tilde{\phi}$ from the floating potential (neglecting temperature fluctuations). The ASDEX data are obtained from a poloidal array of 16 probes separated (in the poloidal direction) by 2 mm and located 1.5 cm outside the last closed flux surface. In ADITYA (major radius $R = 75$ cm, minor radius $a = 25$ cm), the fluctuations are measured by a poloidally oriented rake of ten probes that are 3 mm apart and located 5 mm outside the last closed flux surface. In both experiments, the data have been recorded at a sampling rate of 1 Mhz in Ohmic discharges; the record lengths are, respectively, 20 and 2.05 ms. The simulated density and potential fluctuations used in the letter result from a code describing SOL turbulence driven by the resistive interchange instability [10]. This code uses a pseudospectral method with dealiasing on a 2D grid with a predictor corrector algorithm. Its integration domain is a 256×256 grid of dimensions $128\rho_s$ in both the poloidal and vertical radial directions where ρ_s is the hybrid Larmor radius.

Figure 1 shows the time evolution of potential density fluctuations measured, respectively, in ADITYA and ASDEX, as well as an intensity plot of the simulated density fluctuations at a given time. In all the figures, large (i.e., comparable in size to the thickness of the SOL) and long-lived structures are readily apparent. In ASDEX, these structures have been reported as "fluctuation events" [9]. In ADITYA, the non-Gaussian probability distribution function (PDF) associated with the broadband fluctuations has been interpreted as a signature of intermittency [8]. In both experiments, we find that the structures propagate poloidally in the direction of the ion diamagnetic drift. Finally, in the simulation data, large scale coherent structures have been observed even in the saturated regime of turbulence [10].

The frequency and wave number power spectra of these signals are rather featureless and no predominant periodic structure can be identified. The bicoherence level tends to be small (<2%) but statistically stable, indicating that local quadratic wave couplings are weak. The basic statistical properties of the fluctuations, such as their average lifetime or poloidal extension are as usual inferred from the decay of their cross correlations. Typical correlation times are, respectively, 20, 35, and

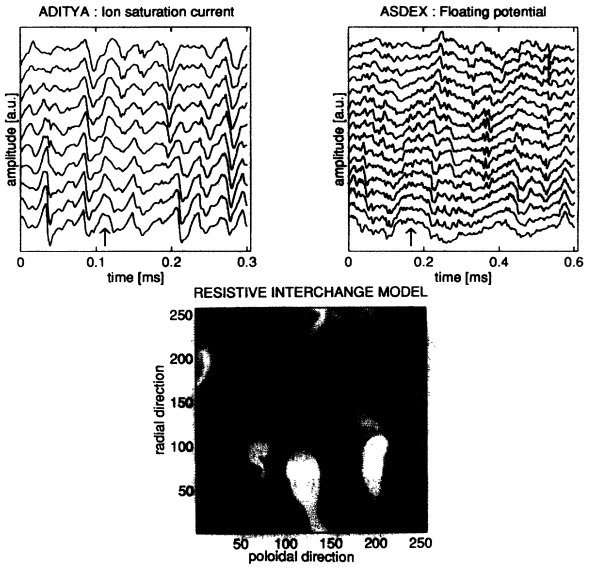

FIG. 1. Time evolution of the ion saturation current measured on ADITYA, the floating potential measured on ASDEX, and 2D intensity plot of the simulated density fluctuations in the poloidal and radial directions (snapshot taken in the saturation regime). The arrows on the figures indicate typical large structures.

50 μs for the ADITYA, ASDEX, and simulation data. Similarly, the average poloidal correlation lengths are, respectively, 3, 2, and 3 cm. Note that these results could be related either to the most unstable mode or to the existence of coherent structures and provide no means for extracting or identifying such structures.

However, the application of the BD to these data leads to the weight distributions that are shown in Fig. 2. The steepness of these distributions is an indication of redundancy in the data sets and means that the salient features are captured by just a few modes. Figure 3 shows the four dominant modes of the ASDEX data, which, together,

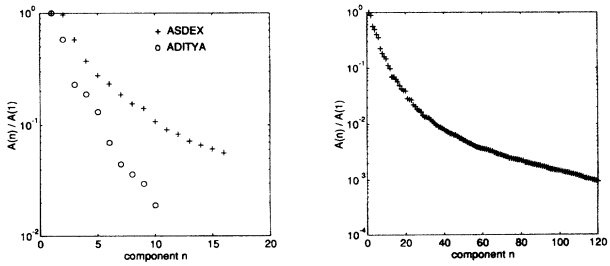

FIG. 2. Distribution of the biorthogonal weights A_n associated with the ADITYA and ASDEX data (left) and the simulation data (right). For the latter only 120 out of the 256 components are shown. The distributions have been normalized for convenience to the value of A_1. The absolute slopes of the distributions depend on the probes spacing and the sampling time, and therefore cannot be meaningfully compared.

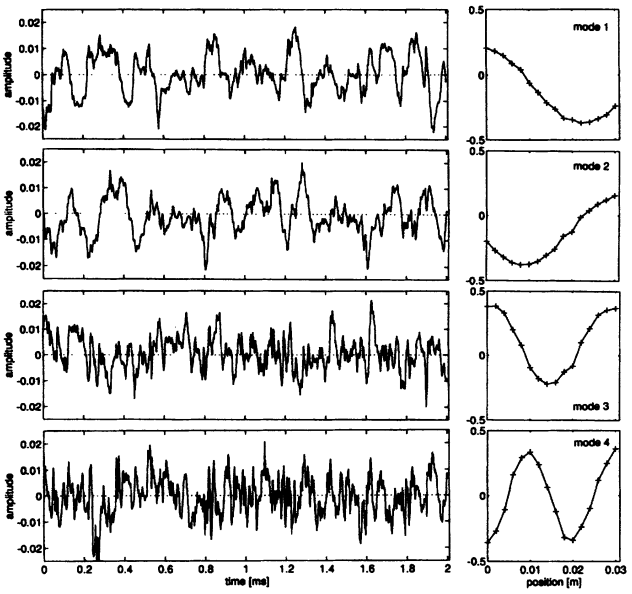

FIG. 3. The four dominant biorthogonal modes of the ASDEX floating potential data. For each mode number, an excerpt of the temporal component (left) and the spatial component (right) are shown.

represent over 94% of the signal variance. A Fourier analysis of the biorthogonal components reveals that the dominant ones also contain the largest scale lengths and longest time scales (Fig. 4). Thus, a significant fraction of the observed fluctuations can be represented in terms of a few modes that are highly correlated in time and in space. This result, and the steepness of the weight distribution, are together a clear signature of the existence of coherent structures.

We must stress at this point that the BD is not equivalent to a 2D Fourier analysis even though the spatial components in Fig. 3 may suggest a close link. In a Fourier analysis, the base functions are prespecified, whereas the biorthogonal components are calculated from the data. In contrast to Fourier modes, the average wave number or frequency of the biorthogonal components does not increase fully linearly with the mode number (Fig. 4). It is precisely this data-adaptive property that allows the BD to identify and isolate in an optimal way the part of the signal that is correlated in time and in space.

The ability of the method to separate different scales (instead of just wavelengths or frequencies) is illustrated in Fig. 5, which shows the ASDEX and simulation data after subtraction of 3 and 10, respectively, of the dominant components. Crude estimates of the numbers of significant components are obtained here from the number of terms needed to explain at least 90% of the variance of the data. A comparison between Figs. 1 and 4 clearly shows that the dominant components capture the large structures and that the subsequent ones represent smaller fluctuating events which end up being randomly distributed.

A direct consequence of these results is that we may use the BD to determine which scales display the strongest intermittency. Since intermittent behavior has been reported for the turbulence observed in SOL of ADITYA [8], we have calculated the PDFs associated with the temporal biorthogonal components of the ADITYA data. The strongest deviation from a Gaussian distribution is observed in the dominant components, thus indicating that large scale structures effectively contribute to intermittency.

Finally, we discuss the contribution of coherent structures to radial particle transport. To this end, the ensemble-averaged particle flux $\Gamma = \langle \tilde{n}\tilde{v}_r \rangle$ is determined, where $\tilde{v}_r$ is the radial component of the convection velocity $\tilde{\mathbf{v}} = \tilde{\mathbf{E}}_\theta \times \mathbf{B}/B^2$, $\tilde{\mathbf{E}}_\theta$ the poloidal component of the fluctuating electric field, and $\mathbf{B}$ the magnetic field. We then define the partial fluxes associated with the biorthogonal components of the density fluctuations as

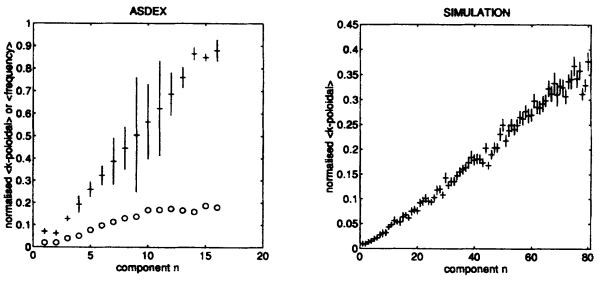

FIG. 4. Average poloidal wave numbers (crosses) and average frequencies (circles) associated with the biorthogonal components of the ASDEX data (left) and average poloidal wave numbers relative to the simulation data (right). The wave numbers (resp. frequencies) are normalized with respect to their Nyquist limit and error bars represent an uncertainty of ± one standard deviation. The dominant modes (i.e., the low order ones) also represent the largest and longest-lived structures.

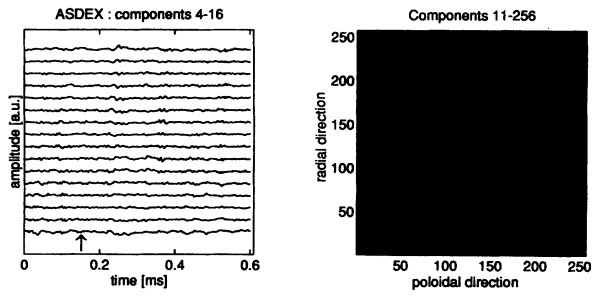

FIG. 5. Reconstruction of the ASDEX and simulation data sets of Fig. 1 after subtraction of their dominant biorthogonal components. Three components have been subtracted from the ASDEX data, ten from the simulation data. Intensity levels (vertical scale) are the same as those used in Fig. 1. Note that the structure marked by an arrow in Fig. 1 has completely disappeared for the ASDEX floating potential signal.

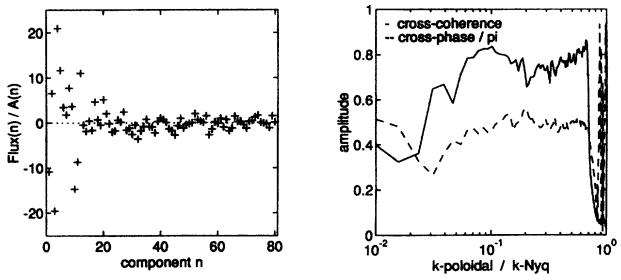

FIG. 6. The partial fluxes Γ_n associated with the biorthogonal components of the simulated density fluctuations (left) and cross phase of density and potential fluctuations (right). Note that each partial flux has been normalized by the corresponding weight A_n of the density. Large fluxes are associated with large coherent structures ($n = 1, \ldots, 20$). The cross phase is 90° at high correlation level.

$\Gamma_n = \langle \tilde{n}_n \tilde{v}_r \rangle$. The partial fluxes associated with the simulation data are displayed in Fig. 6, which reveals their strong concentration in the dominant components. This result also pertains to the experimental data, for the cases where the flux can be inferred from simultaneous ion saturation current and floating potential measurements. A first conclusion is that coherent vortex structures play a dominant role in controlling radial transport. We now turn to the phase relationship between the simulated $\tilde{n}$ and $\tilde{\phi}$, which is given by the argument of the cross-power spectrum of these quantities. The phase angle is found to be close to 90° at large correlation levels, see Fig. 6. We conclude from Fig. 6 that the radial particle transport in the SOL is mainly due to the large scale structures and to their ability to convect the small structures that are essentially concentrated in the steep gradients around the large vortices. Note that a Fourier analysis of the flux provides no means for determining which scales contribute to radial transport because, in contrast with the BD, the power spectrum of the flux does not reveal the dynamical structure of the turbulence. These results are in excellent agreement with experimental observations made on the CCT [2] and ASDEX [9] tokamaks.

In conclusion, the application of the biorthogonal decomposition to Langmuir probe and simulation data, has allowed us to identify, in an unambiguous manner, coherent structures in the SOL of tokamak plasmas. The same conclusions have been reached, using H_α emission data (noninvasive detection technique) from ASDEX. Different spatial or temporal scales (and not frequencies or wavelengths) have been isolated and identified by the BD, which provides an objective statistical test for detecting coherent structures [14]. Using this method, it has been shown that large scale coherent structures effectively contribute to radial particle transport and furthermore explain most of the intermittent behavior observed in the ADITYA tokamak.

These results also reveal a universal behavior in the SOL turbulence of tokamaks, which is characterized by the importance of large scale structures (validation of flute-type models) and the similarity of the properties of these structures, as they are observed on various devices. Finally, we want to stress that the BD is equally appropriate for analyzing 3D turbulence as well. Experiments and numerical simulations are presently being performed to extend this analysis to edge fluctuations (inside the last closed magnetic surface).

S. B. acknowledges stimulating discussions with Professor W. Horton during his visit to the Institute for Fusion Studies (Austin). Dr. R. Jha and Pr. P. K. Kaw are also acknowledged for useful comments. One of us (T. D.) gratefully acknowledges support by the Commission of the European Communities under Grant No. ERB 4001GT920020.

[1] S. J. Zweben, Phys. Fluids **28**, 974 (1985).
[2] G. R. Tynan, Ph.D. thesis, University of California, Los Angeles [University of California Report No. UCLA-PPG-1369, 1991 (unpublished)].
[3] W. Horton, Phys. Rep. **192**, 1 (1990); A. E. Koniges, J. A. Crotinger, and P. H. Diamond, Phys. Fluids B **4**, 2785 (1992).
[4] W. Horton, R. D. Bengston, and P. H. Morrisson, in *Transport, Chaos and Plasma Physics,* edited by S. Benkadda, F. Doveil, and Y. Elskens (World Scientific, Singapore, 1994), p. 200.
[5] A. J. Wootton *et al.,* Phys. Fluids B **2**, 2879 (1990).
[6] H. Johnson, H. L. Pécseli, and J. Trulsen, Phys. Fluids **30**, 2239 (1987); K. J. Biju *et al.,* in Proceedings of the IAEA Technical Meeting on Research Using Small Tokamaks, Serra Negra, 1993 (IAEA, Vienna, to be published).
[7] H. Y. W. Tsui *et al.,* Phys. Rev. Lett. **70**, 2565 (1993).
[8] R. Jha *et al.,* Phys. Rev. Lett. **69**, 1375 (1992).
[9] M. Endler *et al.,* in *Proceedings of the 20th EPS Conference on Controlled Fusion and Plasma Physics, Lisboa, 1993,* edited by J. A. Costa Cabral *et al.* (European Physical Society, Geneva, 1993), Vol. 17C, Pt. II, p. 583.
[10] S. Benkadda, X. Garbet, and A. Verga, Contrib. Plasma. Phys. **34**, 247 (1994).
[11] J. L. Lumley, in *Atmospheric Turbulence and Radio Wave Propagation,* edited by A. M. Yaglom and V. I. Tatarski (Nauka, Moscow, 1967), p. 166.
[12] N. Aubry, R. Guyonnet, and R. Lima, J. Stat. Phys. **64**, 683 (1991); L. Sirovich, Physica (Amsterdam) **37D**, 126 (1989).
[13] T. Dudok de Wit, A. L. Pecquet, J. C. Vallet, and R. Lima (to be published).
[14] This opens the perspective to eliminate from a given spatio-temporal turbulent signal the forcing part and the purely dissipative one while keeping for analysis only large scale structures and the inertial region.

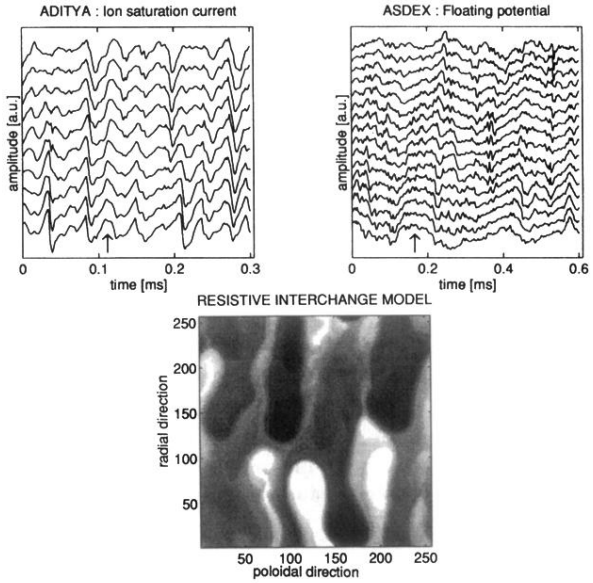

FIG. 1. Time evolution of the ion saturation current measured on ADITYA, the floating potential measured on ASDEX, and 2D intensity plot of the simulated density fluctuations in the poloidal and radial directions (snapshot taken in the saturation regime). The arrows on the figures indicate typical large structures.

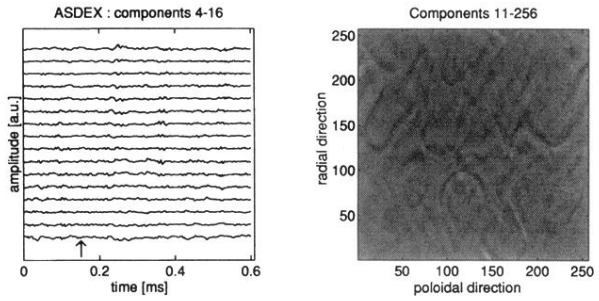

FIG. 5. Reconstruction of the ASDEX and simulation data sets of Fig. 1 after subtraction of their dominant biorthogonal components. Three components have been subtracted from the ASDEX data, ten from the simulation data. Intensity levels (vertical scale) are the same as those used in Fig. 1. Note that the structure marked by an arrow in Fig. 1 has completely disappeared for the ASDEX floating potential signal.